RSC Advances

RSC Advances

ARTICLE

Zeolites and related sorbents with narrow pores for CO_2 separation from flue gas

Ocean Cheung, Niklas Hedin

Adsorbents with small pores are especially relevant for capturing carbon dioxide at large emission sources. Such sorbents could be used potentially to reduce the energy demands for separating carbon dioxide from flue gas as compared with today's technologies. Here, we review the literature for crystalline, inorganic, and potentially inexpensive adsorbents. A number of different adsorbents with narrow pore openings are compared.

Department of Materials and Environmental Chemistry, Berzelii Center EXSELENT on Porous Materials, Arrhenius Laboratory, Stockholm University, S-106 91, Stockholm

niklas.hedin@mmk.su.se

RSC Advances

ARTICLE

General introduction

Adsorption-driven capture of CO_2 from flue gas or natural gas is currently investigated as a potential replacement for absorption processes.[1] For carbon capture and storage (CCS), adsorption-driven capture could ideally reduce the cost for capture of CO_2.[2] The high cost for the capture step of CCS is one of the reasons why it has not been implemented yet. Even though, this review focuses on capture of CO_2 from N_2-rich mixtures, several of the sorbents are relevant for natural gas and biogas upgrading as well.

Adsorbents introduction

Several sorbents classes have been investigated as CO_2 sorbents and include large pore zeolites, metal organic frameworks, amine modified silica materials. Recent reviews of these sorbents include Choi et al.,[1] Li et al.[3] and Moliner et al.[4] In particular, inorganic sorbents with narrow pore openings have advantages when it comes to selectivity for CO_2, uptake of CO_2, stability, and potential cost. Crystalline porous sorbents of the zeolitic kind with narrow pore windows are defined specifically as such compounds with a primary pore window opening encircled by 8 oxygen atoms. Such zeolite-type materials are classified as 8-ring zeolites. The narrow pore windows are of interest because their overall pore dimensions falls close to the effective kinetic diameters of CO_2 and N_2. It is important to note that the effective kinetic diameter of CO_2 is smaller than that of N_2 within porous solids, in contrast to the diameters in gaseous state. Typical values of the effective kinetic diameters within zeolites are 0.33 nm for CO_2 and 0.36 nm for N_2.[5] Effective kinetic diameters here refer to the minimum diameters of CO_2 and N_2 in a porous solid, these quantities will be referred to throughout this review. Notably, these gases have larger molecular diameters in gas phase. In gas phase, CO_2 (0.51 nm) has a larger diameter than N_2 (0.43 nm).[6]

The CO_2-over-N_2 selectivity of a sorbent can have thermodynamic, kinetic and possibly molecular sieving contributions. Thermodynamic contributions towards CO_2 selectivity are related to the significantly lower temperature of condensation (or boiling) for N_2 (77K) as compared with the solidification (or sublimation) temperature of CO_2 (194K). Furthermore, CO_2 also has a higher quadrupole moment (-13.7 × 10^{-24} cm^2) than N_2 (-4.9 × 10^{-26} cm^2). Hence, CO_2 interacts more significantly with the electrical field gradients of the sorbents (such as zeolites) than N_2. It is also important to note that neither CO_2 nor N_2 have dipole moments. The lack of dipole moments means that the interaction between CO_2 or N_2 and the framework's electrical field is not related to permanent dipole moments, but rather to the polarizability of CO_2 and N_2. The kinetic contribution towards selectivity is related to a reduced N_2 diffusivity. N_2 diffusivity can become very low when the size of the pore window aperture approaches the effective kinetic diameter of N_2. For such cases N_2 will be effectively eliminated from sorption when the uptake rate is distinctly slower than the characteristic time of the adsorption process. CO_2, on the other hand, due to the smaller kinetic diameter, will sense less restriction on diffusing throughout the pores of sorbents with narrow pore windows. Under such circumstances kinetics and possibly molecular sieving would contribute to an enhanced CO_2-over-N_2 selectivity. The CO_2-over-N_2 selectivity of different

sorbents can be compared by calculating the separation factor (s). This factor (s) is defined as:

$$s = (q_1/q_2)/(p_1/p_2)$$

where q_1 is the CO_2 uptake at pressure p_1, q_2 is the N_2 uptake at pressure p_2.

Flue gas from a coal burning power plant typically contains up to 15 vol.% of CO_2 (the rest being mainly N_2).[7] In this review we consider a hypothetical flue gas stream which has a pressure feed of 100 kPa and contains 15 vol.% CO_2 (p_1= 15 kPa) , 85 vol.% N_2 (p_2= 85 kPa). The CO_2 uptake of the different sorbents (273K unless otherwise stated) at 15 kPa and N_2 uptake at 85 kPa are listed in Table 1.

The scope of this short review will be narrow and concise and focuses mainly on sorbents based on zeolite and related sorbents with narrow pore windows. The CO_2 separation and sorption capability of these sorbents with narrow pore windows will be explored.

Adsorbents with narrow pore openings

Zeolites

Zeolites are porous and crystalline aluminosilicates that are both naturally occurring and can be synthesized. These covalent oxides of Al and Si form porous structures with interconnected channels or cages. The zeolite frameworks are negatively charged due to the difference in the oxidation states of Al (III) and Si (IV). The negative charges are balanced by exchangeable cations. Even though they share the common chemical formula of $M^{k+}_{x/k}[Al_xSi_yO_{2(x+y)}]$ ZH_2O (where M^+ is the exchangeable cation), there are many different zeolite structures documented to date. These porous zeolites display a significant structural diversity with quite different pore sizes, pore openings, and topologies. The internal pore volume of zeolites is available for adsorption of small molecules and has been utilized in numerous industrial and household applications.

The sorption properties of zeolites were very well studied by Barrer and co-workers in their early work.[8-15] Their work focused mainly on natural zeolites, such as chabazite,[8, 10, 11, 16] mordenite,[10, 13, 15] and analcite.[17, 18] Their studies included size or interaction based selectivities exhibited by zeolites on different sorbates. In addition, they were one of the first to study diffusion of different small organic and inorganic gas molecules in zeolites. We appreciate and acknowledge their work; however, they did not put significant focus on CO_2 sorption. There is a vast amount of previous work on zeolites. Some properties of these materials, including their catalytic[19-21], ion exchange[22-24,25] as well as gas separation/sorption[1, 26] properties. To make this review comprehensive, we focused on the literature related to CO_2 sorption. In specific, a number of zeolite materials with narrow pore windows were considered.

Table 1. CO_2 and N_2 uptake (at 273K, unless otherwise stated) of different narrow pore sorbents at 15 kPa (for CO_2) and 85 kPa (for N_2). The listed values were used to calculate the "selectivity" (*s*) of the adsorbents using $s = (q_1/q_2)/(p_1/p_2)$

Adsorbent	CO₂ uptake at 0.15 bar (mmol/g)	N₂ uptake at 0.85 bar (mmol/g)	Selectivity (s)	Reference
K-CHA	4.0	0.85	27	27
Na-CHA	4.2	1.3	18	27
Li-CHA	4.4	0.53	47	27
Ba-CHA	3.0	1.1	15	27
Mg-CHA	3.4	0.65	30	27
NaA	3.2	0.30	60	28
NaKA (17% K⁺)	2.3	0.02	660	28
MgA	2.4 (298K)	0.25 (298K)	54	29
CaA	4.0 (298K)	0.5 (298K)	45	29
CaA	2.6 (303K)	0.2 (303K)	74	30
H-RHO	1.6 (0.1 bar, 298K)	/	/	31
Li-RHO	3.3 (0.1 bar, 298K)	/	/	31
Na-RHO	3.1 (0.1 bar, 298K)	/	/	31
K-RHO	1.5 (0.1 bar, 298K)	/	/	31
Cs-RHO	0.07 (0.1 bar, 298K)	/	/	31
NaCs-RHO	2.6 (283K)	/	/	32
Zeolite T	2.6 (298K)	0.40 (298K)	37	33
Zeolite T	1.8 (298K)	0.17 (298K)	60	34
Zeolite T	2.7 (288K)	0.40 (288K)	38	34
H-ZK-5	1.1	0.10	62	35
Li-ZK-5	3.9	0.23	96	35
Na-ZK-5	3.4	0.27	71	35
K-ZK-5	3.0	0.23	74	35
Mg-ZK-5	1.9	0.15	72	35
Ca-ZK-5	1.9	0.23	47	35
SAPO-17	1.3	0.31	23	36
SAPO-STA-7	1.7	/	/	37
SAPO-34	1.6	/	/	38
Na-SAPO-34	2.1	/	/	39
Sr-SAPO-34	3.1	/	/	39
SAPO-35	1.8	0.32	33	36
SAPO-56	2.8	0.39	42	36
SAPO-RHO	1.2	0.086	84	36
AlPO-17	0.66	0.14	25	40
AlPO-18	0.52	0.13	22	40
AlPO-25	0.21	0.068	18	40
AlPO-53	0.90	0.031	170	40

Zeolite chabazite can occlude and separate molecules by their size. This property first shown by Barrer and Ibbiston.[17] Zeolite chabazite occluded small straight chain hydrocarbons but branched hydrocarbons were completely excluded. This separation ability was due to the narrow pore windows of chabazite (0.38 x 0.38 nm).[42, 43] More of zeolite chabazite's ability to separate different gas molecules was demonstrated further by Janák et al.[44] and many of the work from Webley's group.[27, 45, 46] Webley and associates observed that CO_2 adsorbed significantly more on all their zeolite chabazite samples when compared with N_2 and CH_4.[27] Zeolite chabazite in its K^+ form (K-CHA) had enhanced ability to separate CO_2 from N_2 and CH_4. The CO_2 uptake of K-CHA, Na-CHA and K-CHA at 113 kPa (273K) was around 5 times higher than the N_2 uptake. Furthermore, at low pressures (1.0 kPa), this ratio (CO_2 adsorbed: N_2 adsorbed, per cavity) reached over 300:1 for K-CHA. They attributed this finding to the fact that CO_2 molecules could penetrate into the windows at low pressures, but the larger N_2 was essentially blocked by the big K^+ cation.
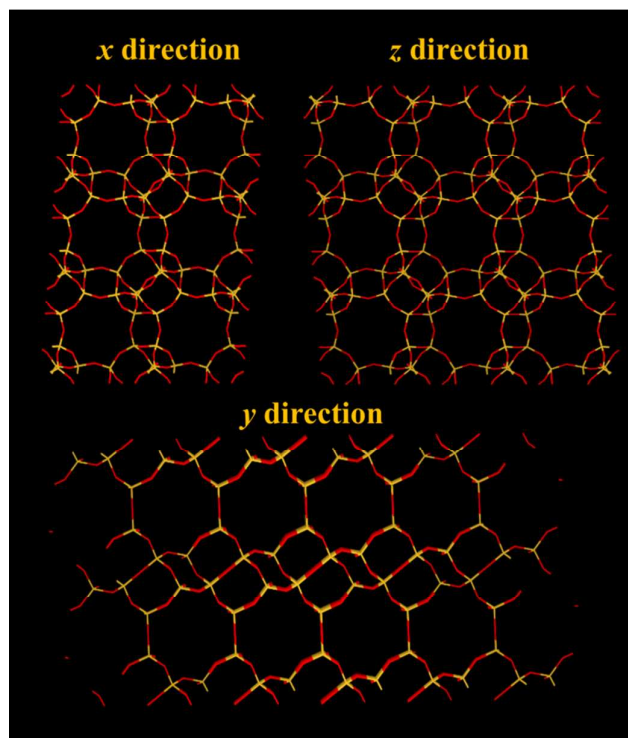
Figure 1. Structure representation of the CHA structure as in chabazite (and SAPO-34). The yellow lines represent Si (or Al) bonds to O, O atoms are represented by red lines
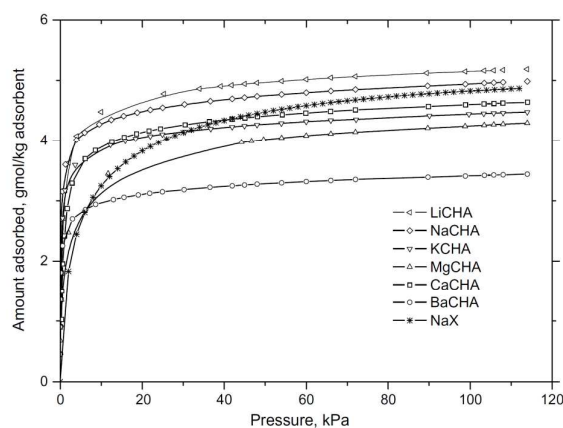
CHA - Zeolite (Chabazite)

The zeolite chabazite (CHA – shown in Figure 1) is one of the most studied zeolites with narrow pore windows. It has a highly accessible porous framework of the 8-ring class with exchangeable cation sites. It exists naturally but can also be synthesized.[41] As the cations can very easily be exchanged, many forms of zeolite chabazite exist. Barrer and associates studied the sorption properties of natural chabazite in detail.[8, 10-12, 17, 41]

Figure 2. CO_2 sorption isotherms of ion exchanged zeolite chabazite at 273K, reproduced with permission.[45]

In terms of the capacity to adsorb CO_2, previous literature shows that zeolites chabazite generally has a high capacity. Inui et al.[47] showed that under pressure swing adsorption (PSA) conditions, zeolite chabazite had high uptake of CO_2 (~3.5 mmol/g) and low irreversible uptake at high pressures (up to 1.1 MPa). Watson et al.[48] demonstrated that the uptake of CO_2 of a natural version of zeolite chabazite could reach over 5 mmol/g at a high pressure (3 MPa, 305 K). Na-CHA and Li-CHA both showed high uptake of CO_2.[45] The equilibrium uptake of CO_2 at 120 kPa (273K) was ~4.4 mmol/g and 4.5 mmol/g for Na-CHA and Li-CHA, respectively. K-CHA, Mg-CHA and Ca-CHA showed CO_2 uptake of ~4.0 mmol/g under the same conditions.[45] Ba-CHA showed a slightly lower uptake of CO_2 (~3.5 mmol/g) under those conditions. The uptake of CO_2 at low and close to zero loading was higher on Ba-CHA than on Li-CHA. The high uptake at low pressures may be related to the strong cation-quadrupole interaction for Ba^{2+} cation and CO_2. This trend illustrates that the cation charge density, the electrical field gradients of the material and the interaction with the quadrupole moment of CO_2 all are important. The original study (Zhang et al.[45]) gave detailed analysis into these observations. Zhang et al.[45] also examined the CO_2 isotherms of different ion exchanged chabazite materials in detail. They considered the dependence of the enthalpy of CO_2 sorption on the cation. For Li-CHA and Na-CHA, the enthalpy of CO_2 sorption increased with increased loading. Their findings agreed with the suggested explanations for the uptake dependencies on the cations, at different pressures. For Ba-CHA, Mg-CHA and K-CHA, the enthalpy of CO_2 sorption dropped at high loading. This was rationalized and related to a decrease of the cation-quadrupole interaction, and that the sorbate-sorbate interaction in these materials was not dominant. In the case of Ca-CHA, the enthalpy of CO_2 sorption stayed fairly constant with an increased loading, indicative of a balanced contribution from sorbate-sorbate interaction and cation-quadrupole interaction. These findings were corroborated by the high uptake of CO_2 observed on Ba-CHA at very low pressures of CO_2.

In short, many of Webley's and associates' work suggested that K-CHA can be a suitable CO_2 sorbent of the zeolite chabazite family. K-CHA showed a higher preferential CO_2 uptake over N_2 than Li-CHA and Na-CHA, as well as a high CO_2 capacity (although slightly lower than Li-CHA). They suggested that the enhanced CO_2 selectivity was due to the large K^+ ion close to the 8MR window blocking N_2 access into the pores.[27] Many other ion exchanged chabazites also showed very good potentials to be CO_2 sorbents. More recently, they proposed a "molecular trapdoor" mechanism to explain the enhanced selectivity of these ion exchanged chabazites.[49, 50] They explained that the very low

uptake (essentially blocked) of bigger molecules such as N_2 and CH_4 was not entirely due to the size effect. Instead, they proposed that CO_2 would interact with the cation strongly enough that the cation deviate from its "normal" site, allowing enough space for CO_2 to enter the pores. Those that have weaker interaction with the cations (N_2, CH_4) do not interact and induce movement of the cation. They concluded that for this mechanism to work properly, the Si/Al ratio needs to be tuned. A low Si:Al ration of around 1.5:1 is preferred to increase the CO_2 selectivity. At this ratio, all "pore aperture doorways" are occupied by cations, which can restrict the adsorption of the N_2 and CH_4.[50] This principle may also be applied to other small pore zeolites such as zeolite A.[50]

LTA - Zeolite A

Zeolite A has been studied extensively, similarly to chabazite. Zeolite A (LTA- Linde Type A) was first reported by Breck in 1956.[51] It is a crystalline aluminosilicate with large cages and narrow pore openings (8-rings) with a number of charge balancing cations. In zeolite A, the Si/Al ratio is strictly 1:1, unlike in chabazite, which can have a higher Si/Al ratio.[45] As a result of the large charge on the framework and the narrow pore openings, the electrical field gradient on zeolite A is typically very high.

Zeolite A (Figure 3) has a cubic structure. The effective size of its windows are heavily dependent on the specific cation present. Monovalent cations tend to populate sites close to the 8-rings, while divalent cations tend to populate sites that do not partially block the 8-rings. Zeolite A with Na^+ as cation has a pore window size of around 0.38 nm and is also called as zeolite 4A due to its pore windows of ~0.38 nm in diameter. This pore window aperture can be adjusted to 0.5 nm or down to 0.3 nm, should the framework contain Ca^{2+} and K^+ ions instead, respectively. Zeolite KA is also called zeolite 3A and zeolite CaA is also called zeolite 5A.
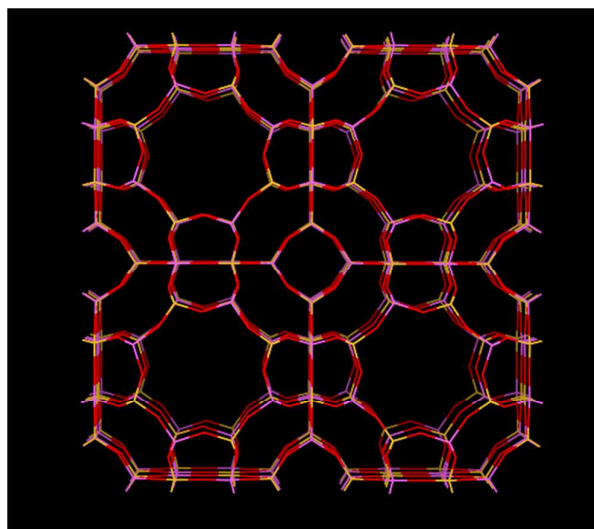
Figure 3. Structure representation of zeolite A, yellow lines represent Si bonds to O, pink lines represent Al bonds to O, O atoms are represented by red lines

The high electrical field gradients of zeolite A may also be responsible to its relatively high uptake of CO_2. In an early study by Harper et al.[52], the capacity to adsorb CO_2 on zeolite NaA was found to be ~6.7 mmol/g at saturation. Those adsorption measurements were carried out at a temperature of 194 K (where CO_2 saturation occurs at atmospheric pressure). At 273 K, they observed that the capacity to adsorb CO_2 was still as high as 4.1 mmol/g (101 kPa). Bae et al.[29] evaluated a range of different

cation exchanged zeolite A for their CO_2/N_2 separation potential. The found that at the relevant pressure range, Ca^{2+} exchanged zeolite A (CaA) had an impressively high CO_2 uptake (~5.0 mmol/g, 298 K) and a CO_2/N_2 selectivity of 250 (predicted by the authors using the ideal adsorption solution theory - IAST). They compared their results with Mg-MOF-74 and found that CaA had a higher volumetric uptake of CO_2 (0.15 bar CO_2, 313K), higher working capacity (based on their TSA study) as well as a longer breakthrough time than MOF-74. Palomino et al.[53] tested zeolite A with high Si:Al ratios (up to 5) and observed that the capacity to adsorb CO_2 varied with the Si:Al ratio. They observed that the CO_2 uptake at 500 kPa (303 K) was the highest for an intermediate Si:Al =2:1. The CO_2 uptake was lower on zeolite A with both lower and higher Si:Al ratios than for a ratio of 2. In addition, they observed that the isosteric heat of CO_2 adsorption (up to 2.5 mmol/g loading) decreased with an increasing Si content. At high Si content, the regenerability of the zeolite A sorbent increased because of the lower heat of CO_2 adsorption.[53] The difference in the heat of adsorption is possibility due to the difference in the number of cations in the zeolite, as CO_2 tends to adsorb more strongly at high energy sites close to the cations (discussed in more details later). Palomino et al.[53] also found that the heat of CH_4 adsorption was not significantly affected by the difference in Si content, but the CO_2/CH_4 selectivity was reduced with increasing Si content. Inui et al.[47] highlighted the high capacities to adsorb CO_2 (3-4 mmol/g, at 1.0-1.2 MPa) of zeolite NaA and CaA in an independent study. Due to the high electrical field gradients, the enthalpy of CO_2 sorption on zeolite A is high. Bae et al.[29] found that CaA had a noticeably higher heat of CO_2 adsorption than NaA, and MgA. The heat of CO_2 adsorption on CaA was around 60 kJ/mol at low loading, and decreased to around 30 kJ/mol with a loading of around 4 mmol/g. They attributed the high heat of CO_2 adsorption to the large number of accessible strong adsorption sites. Delaval and de Lava[54] showed that CO_2 physisorption on zeolite 4A had an enthalpy of around 50 kJ/mol at zero loading. The enthalpy change reduced with increased loading down to ~44 kJ/mol. We previously observed that the enthalpy of CO_2 physisorption on zeolite NaKA was around 37 kJ/mol at non zero loading.[55] The low value we observed may be due to the presence of the big K^+ cations.

As mentioned, the window size of zeolite A can essentially be further adjusted by ion exchange. We recently demonstrated that partially K^+ ion exchanged zeolite NaKA had pore sizes between 0.3 and 0.4 nm. [28] Using this feature of zeolite A, we were able to produce zeolite NaKA with 17% of the cations being K^+, 83% being Na^+. This zeolite, with the reduced pore size, was able to exclude N_2 from sorption onto the material (<0.01 mmol/g, 273 K, 101 kPa). The CO_2-over-N_2 relative uptake of the material reached over 200. The CO_2 capacity of this highly selective zeolite NaKA remained high (3.5 mmol/g, 273 K, 101 kPa). Mace et al.[56] suggested that the high selectivity is not solely due to the bigger cation blocking the bigger sorbates. They concluded that the difference in mobility between Na^+ and K^+ and the higher interaction with CO_2 allowed CO_2 to enter the pores (when the material is not fully K^+ exchanged). Other sorbates, such as N_2, did not have the ability to do so.

The exclusion of N_2 from sorption on zeolite NaKA appeared to be related to its large effective kinetic diameter (0.36 nm). Further reducing the pore window size of zeolite NaKA with additional K^+ ions in the 8-ring, will make the apertures too narrow for CO_2 to pass through, as the effective kinetic diameter of CO_2 is about ~0.33 nm. However, we observed significant capacities to adsorb CO_2 also for zeolite NaKA with a high content of K^+.[28] Different mechanisms have since been proposed to rationalize this unexpected phenomenon. Larin et al.[57] suggested that chemical reactions of CO_2 with the framework atoms would lead to carbonate formation on the K^+ cations near the 8-rings (as K_2CO_3 with one other K^+ cation). They proposed

that such carbonates would reposition the K^+ atoms away from the window aperture. This would have resulted in a wider opening for CO_2 to enter subsequently. Webley and associates,[49, 50] although did not study zeolite A explicitly, proposed "molecular trap door" mechanism for CO_2 entering pores of chabazite when the material had been K^+ exchanged. They stated in their conclusion that they expected to find a similar mechanism on zeolite LTA. The KCHA in their study also had pores that were theoretically blocked for CO_2 to enter. As discussed earlier, they proposed that CO_2 can interact and shift the position of the cation, allowing itself to enter the pores. Recently, Mace et al.[58] presented a procedure using *ab initio* molecular dynamics calculations to access the details of the free energy barriers for diffusion of small gas molecules through 8-ringzeolite windows. By introducing certain spatial constraints, the gas molecule could be steered towards the "rare event" of the diffusion through the pore window of interest, without losing other relevant degrees of freedom. In this work, using this procedure, the free energy barriers of diffusion for CO_2 and N_2 in zeolite NaKA were estimated, investigating the differential molecular sieving effect of the two cation types, Na^+ and K^+, without involving either chemisorption or explicit "molecular trap door" mechanisms. The results were in good qualitative agreement with the experimental results presented by Liu et al.[28] showing a drastic increase in the energy barrier for CO_2 or N_2 to pass a K^+ blocked pore window compared to a Na^+ blocked one, hence strongly supporting the idea of a tunable sieving effect through ion exchange.

The molecular details of CO_2 sorption on zeolite A have also been studied. Jaramillo and Chandross[59] studied CO_2 (physis-) sorption using Gibbs ensemble Monte Carlo simulations. They suggested that CO_2 sorption at low pressures occurred at a single cation Na^+ site around the 6 membered ring windows. CO_2 next adsorbed on a second site where it coordinated with Na^+ from both the 6- and 8-rings. Finally, CO_2 adsorbed on a third site where it coordinated to 3 Na^+ cations (4-,6- and 8-rings). Other evidence of CO_2 adsorption on different sites depending on (CO_2) pressure (or loading) was presented in a study by Delaval and de Lara[54], as well as our recent study on nano-sized zeolite A.[55] These studies involved infrared spectroscopy and observed that the characteristic band for physisorbed CO_2 (v_3 - asymmetric stretching vibration mode) occurred at a higher frequency (2352 cm^{-1}) and downshifted to a lower frequency up on further loading of CO_2. Density Functional Theory (DFT) studies showed that sorption of CO_2 at a low coverage (1 CO_2/α cage) occurred with CO_2 bridging between 2 or 3 cation, irrespective of the size of the cation.[55] Bae et al.[29] determined using a neutron diffraction technique that at low loading of CO_2, there were two adsorption sites on CaA. One of these two sites was located close to the 6-rings where CO_2 could interact with two Ca^{2+} (site A), the other site (site B) was located in the center of the 8-rings (Figure 4).
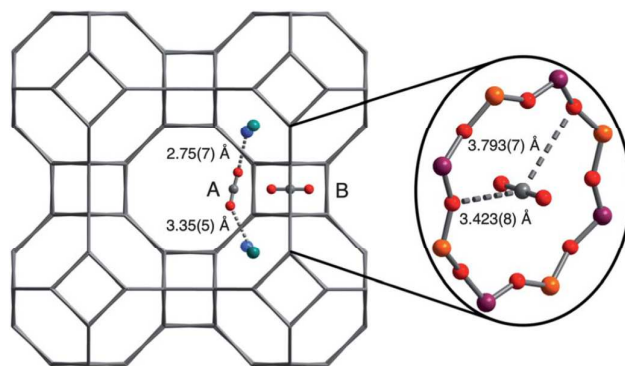

Figure 4. Location of the two CO_2 adsorption sites in zeolite CaA at low loading, as determined using neutron diffraction by Bae et al.[29] reproduced with permission.

Many groups have studied diffusion of CO_2 in zeolite A. This topic has recently been extensively reviewed by Ruthven.[60, 61] Here, we aim to give a short summary of previous work. Yucel and Ruthven[62, 63] concluded in their studies that CO_2 diffusion in zeolite 4A was typically governed by intracrystalline diffusion (although diffusivity/mechanism was hugely dependent on the quality of the crystal). Surprisingly, they observed that zeolites of different origins can have quite different CO_2 diffusivities. They attributed the differences to the subtle changes in the crystal structures and possibility due to the rearrangement of cations. The extent of dehydration could also be of importance, as shown by Kondis and Dranoff.[64] In a recent publication by Ruthven,[60] it was highlighted that the diffusion of sorbates in zeolite A is very complex. Many factors can significant alter the diffusivity of sorbates (such as CO_2) in zeolite A. Zeolite crystals from different sources have very different sorbate diffusivity. The effect of different pre-treatment can also highly alter the diffusivity of sorbates such as CO_2. We recently synthesized nano-sized zeolite A and studied the uptake rates of CO_2 in this material. We found that the apparent diffusion was controlled by a skin layer on the surface of the crystals. We also observed zeolite A from different sources have very different sorbate diffusivity.[55]

RHO type zeolites

RHO type zeolites (Figure 5) have shown interesting and desirable properties as a CO_2 sorbent. RHO type zeolite is a synthetic zeolite with a cubic structure with narrow 8-ring pore openings. Typical Si:Al ratios are around 4 or 5:1. Different forms of this zeolite have shown high capacity to adsorb CO_2. Palomino et al.[32] showed that RHO type zeolite's (as-synthesized, containing Na^+ and Cs^+ cations) capacity to adsorb CO_2 reached >6 mmol/g at a high pressure (~850 kPa, 303 K). At atmospheric pressure (101 kPa, 303 K), its capacity to adsorb CO_2 was still >3 mmol/g. Araki et al.[65] observed a similarly high capacity to adsorb CO_2 on H^+ exchanged RHO type zeolite (obtained by NH_4^+ exchange then calcination of as-synthesized RHO zeolite) that was synthesized using 18-crown-6 (18-C-6) as the organic structural directing agent (SDA). Its capacity to adsorb CO_2 was ~3.5 mmol/g (100 kPa, 298 K). The shape of the CO_2 adsorption isotherm showed a step increase at low pressures. Lozinska et al.[31] independently obtained cation free H-RHO. They showed that the cation free H-RHO adsorbed 3.3 mmol/g of CO_2 at 80 kPa (298 K). The shape of the CO_2 adsorption isotherm on their cation free H-RHO zeolite showed no step-wise increase as observed by Araki et al.[65] The absence of this step-wise increase was due to the higher temperature used for the NH_4^+ exchanged used by Lozinska et al.[31] which lead to a more complete ion exchange. The absence of Na^+ and Cs^+ in the cation free H-RHO zeolite obtained by Lozinska et al.[31] meant that CO_2 did not interact and move the cations (the effect of cation movement is discussed in the next paragraph).
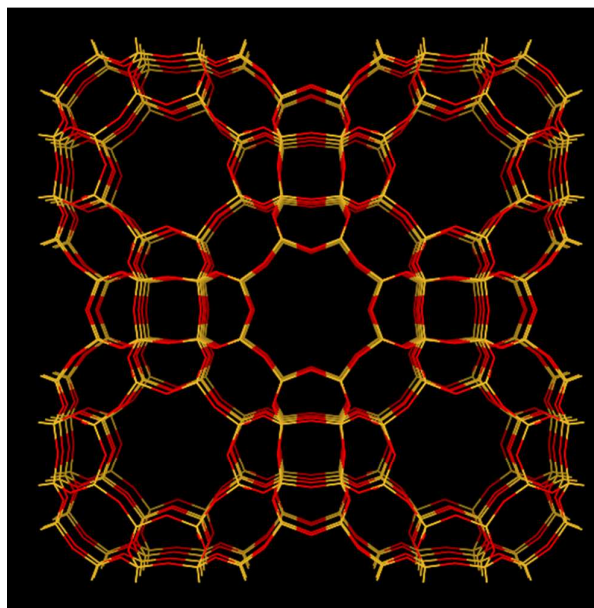
Figure 5. Structure representation of the RHO structure as in RHO type zeolite (and SAPO-RHO). The yellow lines represent Si (or Al) bonds to O, O atoms are represented by red lines

The high CO_2 capacity of RHO type zeolite was in part due to its structure. Araki et al.[65] observed that when the calcination temperature of as-synthesized RHO type zeolite was increased to >673 K, the CO_2 capacity was reduced. They attributed this decreased CO_2 uptake to the phase transformation of the RHO type zeolite at high temperature. At calcination temperatures >773 K, zeolite RHO synthesized with 18-C-6 was no longer stable. Palomino et al.[32] argued that the uptake of CO_2 caused the framework to expand and, hence, the capacity to adsorb CO_2 increased as compared with a non-expanding framework. Such expansion was not observed for N_2 or CH_4, which both were restricted from entering the pores in the first place. Lozinska et al.[31] showed that on cationic forms of RHO type zeolites (not H-RHO), CO_2 interaction with the framework could "move" the cations (these cations otherwise block the pore window that would allow CO_2 to enter) sufficiently to allow CO_2 to enter and adsorb onto cationic RHO type zeolite. The repositioning of the cations changed the unit cell geometry (dimensions) of these zeolites and showed a step increase in the CO_2 adsorptions. The step increase was not observed in the H-RHO zeolite of Lozinska et al.[31] because of the absence of metal (large) cations. The high CO_2 uptake was due to the high pore volume of this zeolite, and not caused by the CO_2 induced repositioning of the cations. The framework effect for many kinds of RHO type zeolites with different cations was studied by Lozinska et al.[31], Lee et al.[66], Corbin et al.[67, 68] Nenoff et al.[69] and Parise et al.[70, 71]

RHO type zeolites appeared to have to a high CO_2 selectivity over other gases such as CH_4 or N_2. Palomino et al.[32] showed that the equilibrium selectivity (CO_2-over-N_2 relative uptake at 100 kPa) of zeolite RHO reached over 75. They attributed the high selectivity to the small pore diameter, as well as the high surface polarity of zeolite RHO.[32] The high selectivity occurs because CO_2 interacts and enables the cations in 8-ring positions to move out of these windows, enabling the CO_2 molecules to enter the pores of RHO-type materials. Cation movement of this kind cannot be induced by other sorbates such as N_2 and CH_4, therefore, adsorption of N_2 and CH_4 on cation RHO zeolites appears as significantly hindered.

Other zeolites

Many other zeolites have also been investigated for their CO_2 sorption and separation capability. Zeolite clinoptilolite also showed some interesting CO_2 sorption properties. Barrer et al.[10, 72] and Inui et al.[47] independently showed a high CO_2 uptake on clinoptilolite at high pressures (3.7 mmol/g at saturation). Barrer and Murphy showed that the CO_2 uptake would increase if the Si/Al ratio of clinoptilolite was increased (to 4.73 mmol/g at saturation when Si:Al reached 70:1).[72] Aguilar-Armenta et al.[73] showed that the CO_2 adsorption kinetics on clinoptilolite was faster than other gases such as O_2, N_2 and CH_4. All the mentioned studies stated that the enthalpy of CO_2 sorption on clinoptilolite was very high (~59 kJ/mol at zero loading)[72] for all ion exchanged forms.[73] Triebe and Tezel[74] specifically mentioned that CO_2 sorption on clinoptilolite was too strong for them to extract interpretable data from the gas chromatography study. The enthalpy of CO_2 sorption was higher than O_2, N_2 and CH_4 as well, giving clinoptilolite enhanced CO_2 selectivity over these other gases. However, the high enthalpy of CO_2 sorption meant that CO_2 was difficult to remove from the material, as demonstrated by Inui et al.[47] This would decrease clinoptilolite's appeal as a CO_2 sorbent under cyclic sorption processes.

Other studies on zeolites with narrow pore opening as CO_2 sorbents include zeolite T and ZK-5. Zeolite T is a narrow pore zeolite with a structure that is the result of the intergrowth of the erionite and offretite structures. The structural details of zeolite T had been clearly examined and discussed in literature.[75, 76] Jiang et al.[34] and Cui et al.[33] studied zeolite T membranes for CO_2 separation from N_2 and CH_4. They found that the narrow pore openings of zeolite T (0.36 x 0.51 nm) could relate to the high selectivity observed. Both studies observed preferential CO_2 uptake on these membranes. The equilibrium CO_2 uptake was just above 3 mmol/g (298 K, atmospheric pressure, note that Cui et al. observed a higher uptake of CO_2 ~3.6 mmol/g under similar conditions).[33, 34] In mixed gas permeation experiments, Cui et al. found that the CO_2/N_2 and CO_2/CH_4 selectivity were 107 and 400, respectively.[33] Zeolite ZK-5 adopts the KFI structure type. It is a high silica zeolite with the Si:Al ratio that varies from 4:1 to 5.1:1. Like other zeolites, it has ion exchange properties.[77] Liu et al.[35] studied zeolite ZK-5 (Figure 6) and the ion exchanged forms of ZK-5. They found that H-ZK-5 had the highest CO_2 uptake at 101 kPa (303 K) of 5.0 mmol/g. On the other hand, they showed that Mg-ZK-5 had high working capacity in the pressure region related to PSA application. Furthermore, Li^+, Na^+, and K^+ exchanged ZK-5 showed better working capacity for CO_2 and higher CO_2 selectivity over N_2 in the pressure regions relevant for vacuum swing adsorption (VSA). Remy et al.[78] synthesized a low silica version of zeolite ZK-5 (LS-KFI) with Si:Al ratio of around 1.6:1. They found that LS-Li- and LS-Na-KFI had higher CO_2 capacity than zeolite Li- and Na-ZK-5 Si:Al = 3.6:1) at low pressures. The higher CO_2 adsorption at low pressures was due to the increased electrostatic interaction between CO_2 and the cations. They also found that zeolite ZK-5 with higher Si content than LS-KFI have higher CO_2 working capacity (in CO_2/CH_4 separation). LS-KFI was more selective for CO_2 over CH_4 than zeolite ZK-5, due to the higher number of cations in LS-KFI than ZK-5. They did not study CO_2 separation from N_2, but similar responses in the CO_2 over N_2 selectivity could be expected on LS-KFI and zeolite that ZK-5.[78]
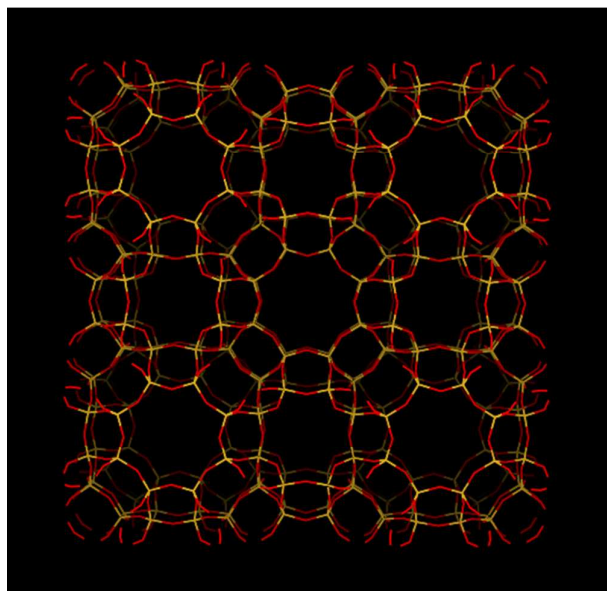
Figure 6. Structure representation of the KFI structure as in zeolite ZK-5. The yellow lines represent Si (or Al) bonds to O, O atoms are represented by red lines

Silicoaluminophosphates and aluminophosphates

Certain crystalline and porous phosphates, in particular silicoaluminophosphates (SAPOs) and aluminosphophates (AlPOs), can have narrow pore openings with 8-rings windows. These classes of phosphates were first synthesized in the early 1980s.[79-81] The structure of AlPO is somewhat similar to microporous silicas.[40] AlPOs are made from covalent oxides of Al and P connected together. Phosphorus has an oxidation state of (V) in the AlPO. This results in a neutral framework with no charge balancing cation, similar to microporous silicas. SAPOs on the other hand are similar to zeolites as they have negatively charged frameworks. The framework structures of SAPO are composed of oxides of Al, Si and P, and the crystallization of SAPOs appears to proceed via an AlPO intermediate.[82, 83] After the formation of such an AlPO intermediate, Si (IV) replaces P (V) in the framework, creating SAPOs. The P replacement by Si creates negative charges on the SAPO framework due to the lower oxidation state of Si (IV). As for zeolites, these charges are balanced by exchangeable cations.

The difference between a neutral and negatively charged framework can be significant. The neutral framework on AlPOs means that the material has a much lower overall electrical field gradient than on SAPOs. These gradients are not as low as those on microporous silicas, due to the more ionic character of the oxides in AlPOs.[84] Consequently, unlike for zeolites, we showed that AlPOs displayed somewhat hydrophobic properties.[40] As expected, the negatively charged framework on SAPOs gives the materials higher electrical field gradients, but not as high as low silica zeolites (e.g. zeolite A). The field gradients also make them more hydrophilic than AlPOs, but less than zeolites.[85] In applications where the gas streams contain a significant partial pressure of water, the difference in hydrophilicity can be of significance.

Both SAPOs and AlPOs can adopt structures that are analogues of zeolites. One of the most studied phosphates, SAPO-34, has the same overall structure as zeolite chabazite (CHA).[86] This compound is easily synthesized and has been in the focus of many studies related to catalysis, ion exchange and gas sorption. It is highly porous with active cation sites. Other phosphates structures, such as AlPO-5 and SAPO-5 (AFI), have no zeolite

analogues (although the pure silica analogue exists). AlPO-5 and SAPO-5 are also widely studied due to their large 12-ring pore channel with a very smooth surface.[87-89] These materials are seen to be potential catalysts in some applications because of high diffusion rate of guest molecules into the pore channel system.

Below different SAPO and AlPO materials with narrow pore openings are reviewed. The previous findings on their CO_2 sorption and separation properties are summarized.

Silicoaluminophosphates with narrow pore openings

A number of SAPO materials with narrow pore openings have been studied for numerous applications. The most notable example is SAPO-34 (CHA).[38, 39, 90-93]

SAPO-34 (structure shown in Figure 1) is commonly studied not only because of its properties, but also due to the easy synthesis and the high purity of the synthetic product. It has been found to be stable under humid atmosphere at temperatures > 373 K, although care must be taken as the adsorption of water generally affect the long term stability of this material.[93] The chabazite framework (Figure 1) also allows for fast diffusion of small gas molecules due to its windows' dimensions (0.38 x 0.38 nm). Many studies have examined the high CO_2 capacity of SAPO-34.[39, 92, 94] The CO_2 uptake on SAPO-34 reached over 3.5 mmol/g at 295 K (101 kPa).[95]

Ion exchanged SAPOs have been studied extensively. One important note on ion exchanged SAPOs is that, unless carefully performed, SAPOs tend to lose their crystallinity upon ion exchange. A possibly reason for the lost in crystallinity is the high concentration of H^+ that is released during ion exchange, which can destroy the SAPO framework. The focus on ion exchanged SAPOs has somewhat been on SAPO-34, particularly Sr-SAPO-34. Arévalo-Hidalgo et al.,[22,23] Hong et al.[38] and Rivera-Ramos et al.[39] are just some of many studies that have found that Sr-SAPO-34 had the best overall adsorption performance for CO_2 of the different SAPO-34 variations. They found that the adsorption capacity for CO_2 was enhanced by the Sr^{2+} cation, especially at low partial pressures of CO_2. Rivera-Ramos et al.[39] argued that Sr-SAPO-34 performed better than the Ce^{3+}, Ti^{3+}, Mg^{2+}, Ca^{2+}, Ag^+ or Na^+ exchanged SAPO-34. They suggested that the Sr^{2+} cations are easily accessible but without causing any transport resistance or pore blocking. The low stability of Ce^{3+} and Ti^{3+} (and Ti^{4+}) cations for ion exchange on SAPOs/zeolites needs to be considered. On the other hand, they assumed that Ce^{3+} and Ti^{3+} cations blocked the pores by occupying the S'III site, giving the variations very low CO_2 uptake. Arévalo-Hidalgo et al.[92] had similar observations for Na-SAPO-34 and Ba-SAPO-34. They too suggested that the cation sites for Sr^{2+} (and Ba^{2+}) are located in a position where CO_2 interaction will consequently become strong.

Takeguchi et al.[81] incorporated Cu^{2+}, Fe^{3+}, Ni^{2+} into the SAPO-34 (CHA) framework to concentrate and separate CO_2 from N_2-diluted gaseous mixture in a PSA apparatus. They observed that SAPO-34 and, in particular, Ni-SAPO-34 have high CO_2 separation and uptake capacities. Ni-SAPO-34 was able to concentrate CO_2 from a gas stream with a CO_2 concentration of 2.9% up to 84.4% with a high CO_2 recovery up to 33%. They compared these Ni incorporated SAPO-34 with zeolite ZSM-34 (silica version of zeolite T, mixed ERI and OFF phases) and SAPO-20 (a 6-ring material). They concluded that metal incorporated SAPO-34 had the best properties for CO_2 separation from a mixture with N_2, when compared with the other materials they studied.

Several groups synthesized SAPO-34 onto membranes for gas separation testing. Different gas pairs were investigated for such inorganic membranes of SAPO-34 including CO_2/CH_4, H_2/CH_4,

CO_2/N_2, N_2/CH_4 and other light gas mixtures.[38, 96-99] For non ion exchanged SAPO-34 membrane, the difference in diffusivities of different gases allowed the membranes to show high selectivity towards CO_2 over N_2 and CH_4.[95]

Separate from ion exchange, Venna and Carreon[91] functionalized SAPO-34 on a membrane with amines (ethylenediamine, hexylamine and octylamine). They tested the properties of these amine impregnated SAPO-34 membranes with respect to their properties related to separation of CO_2. Amine functionalization on such small pore materials has not been studied extensively. They observed with low amine loading, there was an improvement on the CO_2 uptake due to CO_2 interaction with amine groups. At high amine (ethylenediamine) loading, the capacity to CO_2 adsorption and transport were adversely affected. The functionalized material, with low amine loading, showed steeper CO_2 isotherms at low pressures and a higher equilibrium uptake overall.
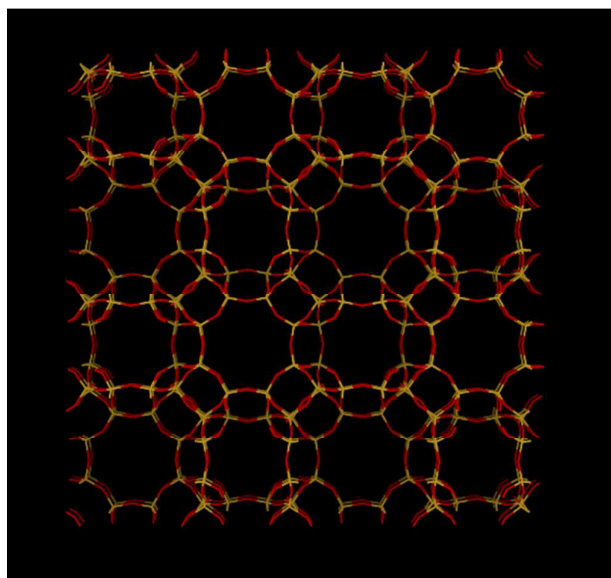
Figure 7. Structure representation of SAPO-STA-7 (SAV) The yellow lines represent Si (P or Al) bonds to O, O atoms are represented by red lines
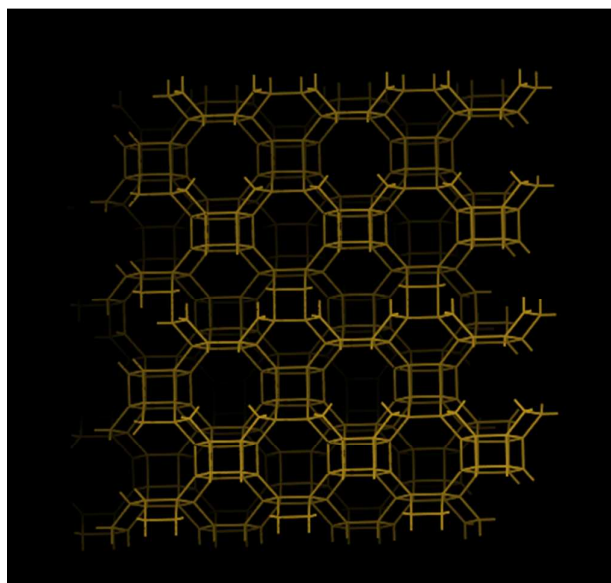
Figure 8. Structure representation of SAPO-35 (LEV), the yellow lines represent covalent bonds between two metal (Si, Al or P) atoms (bridging O atoms), oxygen atoms are purposely omitted in order to show the pore system more clearly
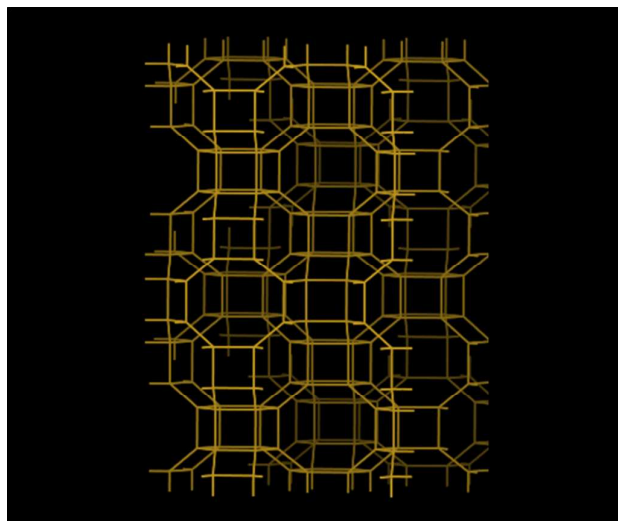
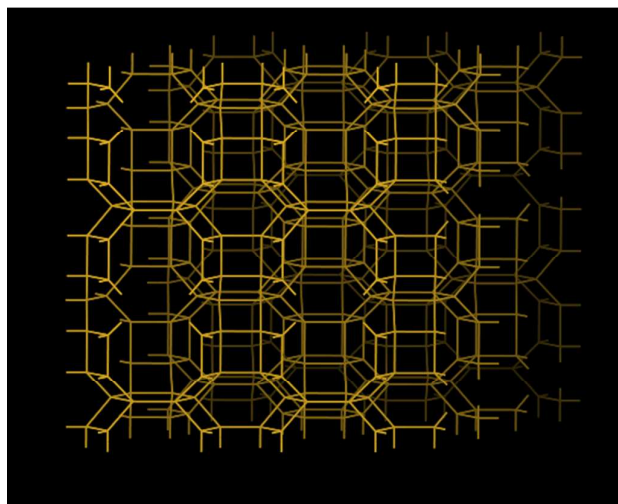**Figure 9**. Structure representation of SAPO-56 (AFX), the yellow lines represent covalent bonds between two metal (Si, Al or P) atoms (bridging O atoms), oxygen atoms are purposely omitted in order to show the pore system more clearly

Figure 10. Structure representation of SAPO-17/AlPO-17 (ERI), the yellow lines represent covalent bonds between two metal (Si, Al or P) atoms (bridging O atoms), oxygen atoms are purposely omitted in order to show the pore system more clearly

Other SAPO materials with narrow pore openings have not been studied as much as SAPO-34, but some of the studied SAPOs display interesting CO_2 separation properties. SAPO-STA-7 (SAV, Figure 7), a material first synthesized by Castro at al. [37], showed very high CO_2 uptake at high pressures. They studied the molecular and thermodynamic details of CO_2 sorption. In contrast to AlPO-18 (discussed later), CO_2 has two different adsorption sites on SAPO-STA-7. The heat of CO_2 sorption was found to decrease with increased loading (from ~38 to ~25 kJ/mol). They attributed this large change in heat to that the adsorption sites associated with a high heat of CO_2 sorption were occupied first. When these sites were fully occupied, CO_2 began to adsorb on less energetically favorable sites. We drew very similar conclusions for SAPO-35 (Figure 8) and SAPO-56 (Figure 9) using results from in situ IR spectroscopy. [36] In that

study, we found that CO_2 sorption first occurred on high energy (strong) Lewis acid sites, where actually CO_2 acted as a Lewis base. Su et al. [100] studied SAPO-RHO (referred DNL-6, Figure 5) and found that CO_2 uptake was enhanced by the number of acid sites. They found that SAPO-RHO had the highest CO_2 uptake at a medium level of Si incorporation (Si:Al 0.37:1). This level of Si incorporation corresponded to the highest concentration of acid sites. In general, CO_2 sorption took place on the lower energy sites when the loading increased. This trend was clearly visible from the in situ IR spectra of CO_2 sorption on both SAPO-35 and SAPO-56. The asymmetric stretching vibration mode of adsorbed CO_2 downshifted from 2357 cm^{-1} to 2345 cm^{-1} with increased CO_2 loading (frequencies for SAPO-56). In the same study, we studied a range of SAPO materials with narrow pore openings. SAPO-56 had very high CO_2 capacity at 5.5 mmol/g at 273 K (101 kPa), this level of uptake was very comparable to the commercially available zeolite 13X sorbent. Other SAPOs, including SAPO-17 (ERI, Figure 10), SAPO-35 and SAPO-RHO, all had respectable levels of equilibrium CO_2 uptake at 237 K, 101 kPa (3.3 mmol/g, 3.6 mmol/g and 3.6 mmol/g, respectively). As expected with SAPOs with their lower electrical field gradients (than zeolites'), the shapes of the CO_2 isotherms were less steep at low pressures. These less steep isotherms were partly due to the lower amount of chemisorbed CO_2 on SAPOs than on zeolites such as zeolite NaA. Still, the equilibrium CO_2/N_2 selectivities of these SAPOs were not low. These phosphates were also found to be less hydrophilic than zeolite 13X, as shown by the shape of the water adsorption isotherm at low relative pressures. This tendency means that under slightly moist conditions, SAPO material will be less sensitive to the presence of water than typical zeolites. [36] Hydrophilicity can be an important property of a CO_2 sorbent, as the use of a non-water sensitive sorbent will significantly reduce the cost of drying the gas stream.

Aluminophosphates with narrow pore openings

The low hydrophilicity is perhaps the most predominant feature of AlPO materials. These materials, with the lack of framework negative charges and charge balancing cations, have very low electrical field gradients. On the other hand, the electrical field gradients of AlPOs are still higher than microporous silica. The lower field gradients reduce the interaction between the material and water, making AlPOs somewhat hydrophobic. These properties was observed by us in our study related to a range of AlPOs with narrow pore openings, including AlPO-17 (ERI-Figure 10), AlPO-18 (AEI), AlPO-21 (AWW), AlPO-25 (ATV) and AlPO-53 (AEN). The structures of these AlPOs are shown in Figure 11. The water adsorption isotherms showed very little water uptake at low relative pressures, particularly for AlPO-53. [40]

RSC Advances Accepted Manuscript
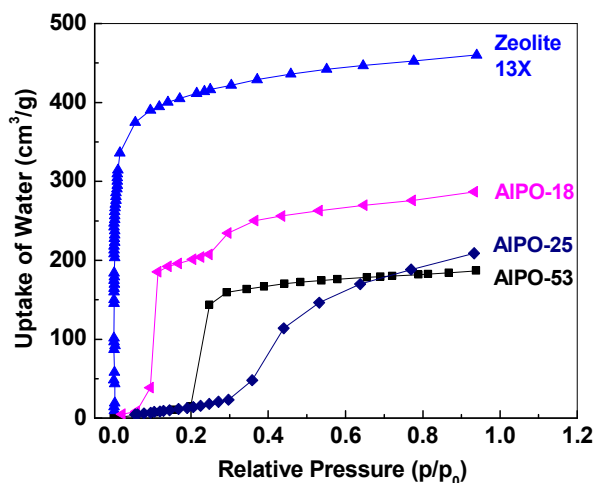
Figure 11. Water adsorption isotherms of various narrow pore AlPOs at 293K, compared with zeolite 13X
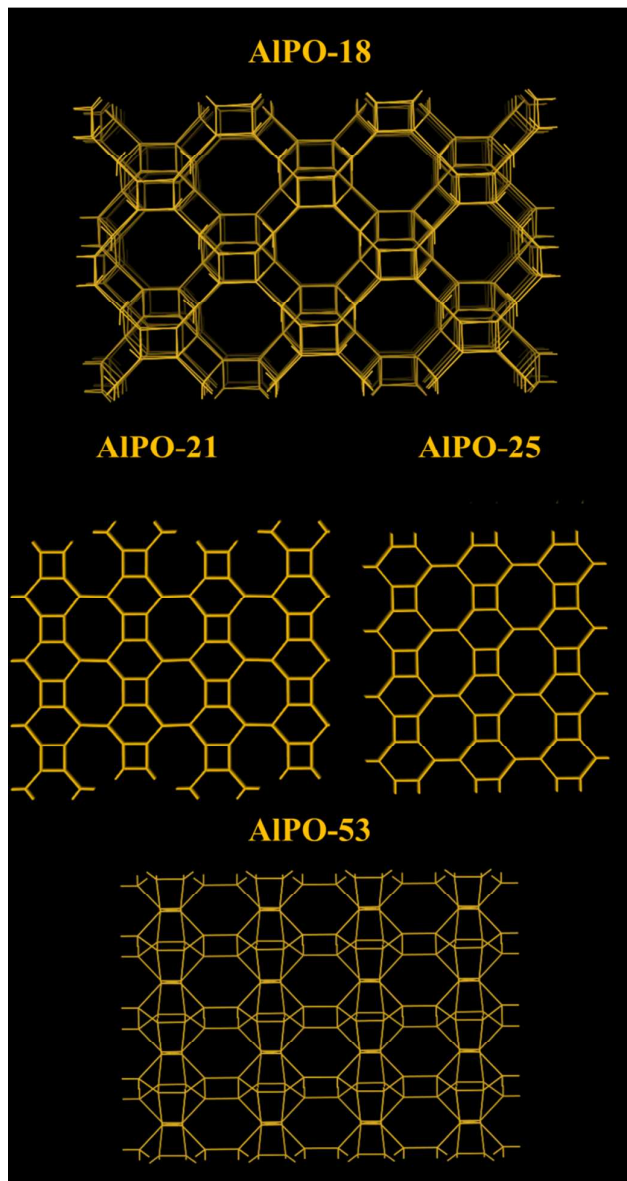
Figure 12. Structure representation of AlPO-18 (AEI), AlPO-21 (AWO), AlPO-25 (ATV) and AlPO-53 (AEN), the yellow lines represent covalent bonds between two metal (Al or P) atoms (bridging O atoms), oxygen atoms are purposely omitted in order to show the pore system more clearly. Note that AlPO-21 transforms to AlPO-25 upon calcination

The effects of the low electrical field gradients of AlPOs were not limited to the water uptake. AlPO-17, which has the same basic structure as SAPO-17, exhibited a lower equilibrium uptake of CO_2 (at 101kPa and 273 K).[36, 40] The uptake of CO_2 of AlPO-17 was 2.3 mmol/g under these conditions (as compared to 3.3 mmol/g for SAPO-17). The lower uptake was in part, related to the lack of chemisorbed CO_2 because of the absence cation sites. The shape of the CO_2 isotherm of AlPO-17 had a more linear respond than its SAPO counterpart.

The equilibrium uptakes of CO_2 of the other AlPOs were still significant, although not as high as for SAPOs or zeolites. This difference could be the reason why AlPOs are not as well studied as CO_2 sorbents. The main explanation to the lower uptake of CO_2 on AlPOs at the studied conditions is the weaker interaction between their frameworks and CO_2. Nevertheless, some groups have studied AlPO-18 as a CO_2 sorbent. Carreon et al.[101] synthesized a AlPO-18 membrane for CO_2 separation. The AlPO-18 membrane offered high selectivities for CO_2/N_2 (19) and CO_2/CH_4 (up to 59) with a high CO_2 permance of ~ 6.4 x 10^{-8} mol s Pa/m^2 (295K). Wright and co-workers [102] studied AlPO-18 both using computational and experimental approaches. They compared the shapes of the CO_2 isotherms for AlPO-18 and a SAPO material (STA-7). The isotherms showed a much gentler slope on AlPO-18 in the low pressure region. This shape strongly suggested that AlPOs had lower enthalpy of sorption for CO_2 than SAPOs. CO_2 essentially experiences AlPOs as materials with relatively homogeneous surfaces. On AlPOs, there are no high energy adsorption sites, as one would expect to find on zeolites or even SAPOs. This absence was indicated by the increasing trend for the enthalpy of sorption with increased loading of CO_2. Sorption did not first occur on any particular sites, and, hence, the enthalpy change during sorption was very similar or all sites. The increased enthalpy of sorption at high loadings was related to CO_2 interacting with other already adsorbed molecules of CO_2.

Interestingly, AlPOs have the ability to retain almost all of its capacity to adsorption of CO_2 under cyclic adsorption conditions.[40] This retained capacity has been related to the lack of chemisorption and high energy physisorption sites. After 5 adsorption cycles, AlPO-53 and AlPO-17 retained >99% of their original capacity. This would suggest that these materials would have a longer life time over many cycles. Furthermore, due to the more linear shape of the CO_2 adsorption isotherms of AlPOs as compared with SAPOs and zeolites, the AlPOs could be comparably more suitable for certain PSA based separations. The removal of CO_2 from AlPOs during desorption can be effective and lead to a high working capacity in some industrial applications.

Microporous silicas with narrow pore openings

In the previous section, we considered the low electrical field gradients on AlPOs and that those had both advantages and disadvantages when it comes to their gas (and water) sorption properties. Microporous silicas belong to a related class of materials with low electrical field gradients. These silicas are essentially three dimensional covalent and crystalline SiO_2 with internal pores. Hence, the framework of microporous contains Si and O atoms only. The frameworks are neutral with no charge balancing cations. When compared with AlPOs, the electrical field gradients of microporous silicas are even lower, as the surface of the material is much more homogenous than AlPOs (with its two different electropositive atoms).[28]

Because of the low electrical field gradients, the porous SiO_2 do not interact strongly with sorbates via the quadrupole-"electrical field gradient" mechanism. Despite of that, the capacity of CO_2 sorption on certain microporous silicas can still be rather significant. Maghsoudi et al.[103] studied Si-CHA and found that the uptake of CO_2 reached ~2 mmol/g (at 298 K and atmospheric pressures). Himeno et al.[104] found that at higher pressure (3 MPa, 298 K), the uptake of CO_2 on Si-CHA reached around 2.7 mmol/g. The uptake was less than that of H_2S but significantly higher than those of CH_4 and N_2 at all studied pressures.[103] Maghsoudi et al. observed that its uptake of CO_2 was 4.1 times higher than the uptake of CH_4 at 100 kPa and 298 K.[104] Miyamoto et al.[105] observed that its uptake of CO_2 was 19 times higher than its uptake of N_2 at 75 kPa and 313 K and 5 times greater at high pressures (800 kPa, 313 K). With a CO_2-N_2 (equimolar) mixed gas, the uptake of N_2 of the Si-CHA membrane became negligible even at high pressures (1.2 MPa).[105] Similar results were observed on Si-DDR. Himeno et al.[104] and van den Bergh et al.[106, 107] showed in their studies that the

uptake of CO_2 of membranes of Si-DDR membrane was 2-3 mmol/g at 273 K (120 kPa) and very high CO_2 selectivity over N_2 and CH_4 (slight variations between the different studies, probably due to the different membranes). Separate permanence studies have shown that the CO_2 selectivity over N_2 and CH_4 can reach 3000 (or around 40 for a CO_2, N_2 and CH_4 mixture).[106, 107]

The high CO_2 selectivity observed was related to the sorbent-sorbate interaction. For a non-polar material with as low electrical field gradient as microporous SiO_2, the adsorption of sorbate is mainly based on dispersion and repulsion interactions. CO_2 with its significant quadrupole moment is more easily polarizable than N_2 and CH_4. The quadrupole on CO_2 can induce polarity on the SiO_2 framework, increasing the sorbent-sorbate interaction.[103] Another reason for this high selectivity is due to the window size of the materials, in particular Si-DDR. van den Bergh et al. concluded that the high selectivity was due to 3 different factors; steric effect (and consequently a kinetic effect) introduced by the small window opening of Si-DDR, competitive adsorption effect and the interaction between sorbent and sorbate, the latter two are very much enhanced for sorption of CO_2.[107]

Due to the comparably low interaction between CO_2 and the crystalline SiO_2 framework, the enthalpy of CO_2 sorption on these materials is low. In addition, these sorbents do not chemisorb CO_2. Maghsoudi et al.[103] found that enthalpy of CO_2 sorption on Si-CHA was 21 kJ/mol (non-zero loading), which was significantly lower than on zeolites and phosphates. Himeno et al. established that enthalpy of CO_2 sorption on Si-DDR was even lower (18.2 kJ/mol at non zero loading), lower than some other crystalline and microporous SiO_2 (~32 kJ/mol).[104, 108]

Titanium silicates (Titanosilicates) – ETS-4

Titanium silicate ETS-4 is built from covalently linked oxides of Ti and Si. It is a structure analogue of the mineral zorite,[109] with a 3 dimensional framework. It has a 12-ring channels running along the crystallographic *z* axis and 8-ring channels running along the *y* axis (Figure 13). Although not covered by this review, the ion exchange[110, 111] and catalytic[112] properties of ETS-4s were found to be impressive. The as synthesized form of ETS-4, usually Na-ETS-4, becomes unstable when dehydrated. Some cation exchanged forms (mainly with divalent cations) of ETS-4 are more stable, as demonstrated by Anderson and Kuznicki et al.[109, 113] At high degrees of dehydration, ETS-4 often transforms into a related phase called as CTS-1 (contracted titanosilicate-1).[113, 114] Nevertheless, the pore size of CTS-1 can be controlled by dehydration under which it contracts. The contraction is not easily reversible. Nair et al. showed that dehydration of Sr-ETS-4 can "continuously vary(ing) the effective pore dimension". Kuznicki et al, showed that Sr^{2+} exchanged ETS-4 can be used for separation CO_2 from CH_4, the material has since be put into application and carries a name of "Molecule Gate".[113-115] As shown separately by Park et al.[116] the CO_2 uptake of Sr-ETS-4 and other forms of ETS-4 varied significantly depending on the dehydration temperature. In their study, Ca-ETS-4 dehydrated at 373 K for 8 hours showed the highest uptake of ~2.2 mmol/g (101 kPa, 298 K) of Ca, Sr and Ba-ETS-4 (Figure 14). We are currently studying a range of ETS-4s in detail, paying particular attention to the transformation from ETS-4 and CTS-1. Anson et al.[117] innovatively incorporated halogen atoms onto the framework of some ETS-4s during the synthesis step. The large halogen atoms were placed around the 8-ring windows and increased the CO_2 over CH_4 selectivity.
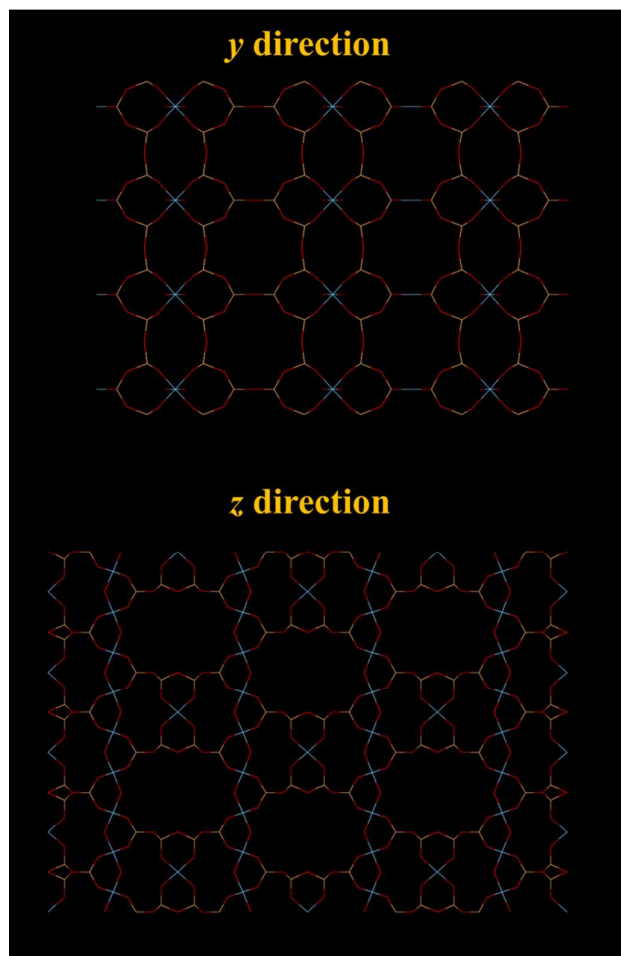
Figure 13. Structural representation of ETS-4, The yellow lines represent Si bonds to O, light blue lines represent Ti bonds to O, O atoms are represented by red lines. CTS-1 is a disordered, contracted version of ETS-4, the basic structure of the two appeared to be the same
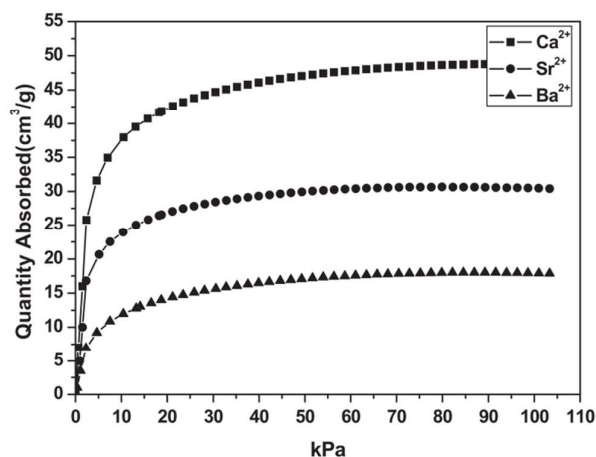
Figure 14. CO_2 adsorption isotherms of Ca, Sr and Ba-ETS-4 at 298 K, samples prepared at 373 K. Reproduced with permission [116]

Conclusion and outlook

A wide range of potential sorbents is available for the purpose of CO_2 capture. Here, we explored some of the most studied

inorganic porous sorbents with narrow pore openings. Each of the sorbents discussed here, of course, has its own advantages and drawbacks. Zeolites have been very thoroughly studied up to now and continuous efforts are being made. A main advantage of zeolites is the cost of manufacture. Both zeolite chabazite and zeolite A are commercially available and the properties of these materials can be easily tuned. Studies have found that zeolites offer high uptake of CO_2 and certain variations have very high selectivity. The high electrical field gradients of zeolites are partly responsible for these features. Unfortunately, zeolites can adsorb CO_2 very strongly, reducing the ease for their use in cyclic processes. Furthermore, zeolites are also hydrophilic. All silica zeolites (microporous silicas) can overcome both these problems. The low electrical field gradient weakens the strength of CO_2 sorption and makes such silicas hydrophobic, yet still offering very high selectivity. As a result, microporous silicas can have good cyclic capacity for CO_2. The comparatively low uptake of CO_2 and somewhat tedious synthesis, as well as the high cost of mass manufacture are the major drawbacks of silicas. Should more efforts be put into developing zeolite based sorbents, the focus should be on simplifying and reducing the cost of producing microporous silicas.

A middle way between zeolites and microporous silicas would direct towards the phoshpates materials. SAPOs offer equally high capacity for adsorption of CO_2 as zeolites at relevant pressures. Their weaker electrical field gradients and lower number of cations result in highly reversible uptake of CO_2 and lower sensitivity towards water. AlPOs are somewhat similar to SAPOs, with even lower sensitivity towards water, but the uptake of CO_2 is also noticeably reduced at the relevant temperatures and pressures. They offer an impressive cyclic capacity; Over 99% of the capacity to adsorption of CO_2 was retained by AlPO-53 and AlPO-17 after 5 adsorption cycles. Even though AlPOs can be costly to synthesise, the potentially long lifetime may be an argument to develop these materials further.

A titanium silicate (ETS-4) has also been well studied as a CO_2 sorbent and is already used in application for biogas upgrading. The tuneable pore size (by dehydration) is an attractive feature of using this material in application. ETS-4 has many potentials, further development of ETS-4 could provide very valuable outcome.

Taken all together, many of these narrow pore adsorbents have shown potentials for applications in CO_2 separation, but several problems are yet to be overcome. We believe that intensified collaborations, between engineering groups and chemistry/physics groups would be especially beneficial for the further development of these sorbents.

Acknowledgement

Notes and references

1.   S. Choi, J. H. Drese and C. W. Jones, *ChemSusChem*, 2009, **2**, 796-854.
2.   M. M. F. Hasan, E. L. First and C. A. Floudas, *Phys. Chem. Chem. Phys.*, 2013, **15**, 17601-17618.
3.   J. Li, Y. Ma, M. C. McCarthy, J. Sculley, J. Yu, H.-K. Jeong, P. B. Balbuena and H.-C. Zhou, *Coord. Chem. Rev.*, 2011, **255**, 1791-1823.
4.   M. Moliner, C. Martínez and A. Corma, *Chem. Mater.*, 2013, **26**, 246-258.
5.   R. C. Weast, *CRC Handbook of Chemistry and Physics*, CRC Press, 1967.
6.   B. Poling, J. Prausnitz and J. O. Connell, *The Properties of Gases and Liquids*, Mcgraw-hill, 2000.
7.   X. Xu, C. Song, R. Wincek, J. M. Andresen, B. G. Miller and A. W. Scaroni, *Fuel Chem. Div. Preprints*, 2003, **48**, 162-163.
8.   R. M. Barrer, *Discuss. Faraday Soc.*, 1949, **7**, 135-141.
9.   R. M. Barrer, *J. Colloid Interface Sci.*, 1966, **21**, 415-434.
10. R. M. Barrer and D. W. Brook, *Trans. Faraday Soc*, 1953, **49**, 1049-1059.
11. R. M. Barrer and D. W. Brook, *Trans. Faraday Soc*, 1953, **49**, 940-948.
12. R. M. Barrer and B. E. F. Fender, *J. Phys. Chem. Solids*, 1961, **21**, 1-11.
13. R. M. Barrer and L. V. Rees, *Trans. Faraday Soc*, 1954, **50**, 852-863.
14. R. M. Barrer and D. W. Riley, *J. Chem. Soc.*, 1948, 133-143.
15. R. M. Barrer and A. B. Robins, *Trans. Faraday Soc*, 1953, **49**, 929-939.
16. R. M. Barrer and D. W. Riley, *Trans. Faraday Soc*, 1950, **46**, 853-861.
17. R. M. Barrer and D. A. Ibbitson, *Trans. Faraday Soc*, 1944, **40**, 195-206.
18. R. M. Barrer, *Proc. R. Soc. London, A*, 1938, **167**, 392-420.
19. S. S. Shepelev and K. G. Ione, *React. Kinet. Catal. Lett.*, 1983, **23**, 319-322.
20. M. Minachev Kh and I. Isakov Ya, in *Molecular Sieves*, American Chemical Society, 1973, pp. 451-460.
21. I. I. Ivanova and E. E. Knyazeva, *Chem. Soc. Rev.*, 2013, **42**, 3671-3688.
22. A. Hedström, *J. Environ. Eng.*, 2001, **127**, 673-681.
23. S. E. Bailey, T. J. Olin, R. M. Bricka and D. D. Adrian, *Water Res.*, 1999, **33**, 2469-2479.
24. S. Wang and Y. Peng, *Chem. Eng. J. (Lausanne)*, 2010, **156**, 11-24.
25. P. Misaelides, *Micro. Meso. Mater.*, 2011, **144**, 15-18.
26. N. Hedin, L. Andersson, L. Bergström and J. Yan, *Appl. Energy*, 2013, **104**, 418-433.
27. F. N. Ridha and P. A. Webley, *Sep. Purif. Technol.*, 2009, **67**, 336-343.
28. Q. Liu, A. Mace, Z. Bacsik, J. Sun, A. Laaksonen and N. Hedin, *Chem. Comm.*, 2010, **46**, 4502-4504.
29. T.-H. Bae, M. R. Hudson, J. A. Mason, W. L. Queen, J. J. Dutton, K. Sumida, K. J. Micklash, S. S. Kaye, C. M. Brown and J. R. Long, *Energy Enviro. Sci.*, 2013, **6**, 128-138.
30. Z. Liu, C. A. Grande, P. Li, J. Yu and A. E. Rodrigues, *Sep. Sci. Technol.*, 2011, **46**, 434-451.
31. M. M. Lozinska, E. Mangano, J. P. S. Mowat, A. M. Shepherd, R. F. Howe, S. P. Thompson, J. E. Parker, S. Brandani and P. A. Wright, *J. Am. Chem. Soc.*, 2012, **134**, 17628-17642.
32. M. Palomino, A. Corma, J. L. Jorda, F. Rey and S. Valencia, *Chem. Comm.*, 2012, **48**, 215-217.

33. Y. Cui, H. Kita and K. Okamoto, *J. Mater. Chem.*, 2004, **14**, 924-932.

34. Q. Jiang, J. Rentschler, G. Sethia, S. Weinman, R. Perrone and K. Liu, *Chem. Eng. J. (Lausanne)*, 2013, **230**, 380-388.

35. Q. Liu, T. Pham, M. D. Porosoff and R. F. Lobo, *ChemSusChem*, 2012, **5**, 2237-2242.

36. O. Cheung, Q. Liu, Z. Bacsik and N. Hedin, *Micro. Meso. Mater.*, 2012, **156**, 90-96.

37. M. Castro, R. Garcia, S. J. Warrender, A. M. Z. Slawin, P. A. Wright, P. A. Cox, A. Fecant, C. Mellot-Draznieks and N. Bats, *Chem. Comm.*, 2007, 3470-3472.

38. M. Hong, S. Li, H. F. Funke, J. L. Falconer and R. D. Noble, *Micro. Meso. Mater.*, 2007, **106**, 140-146.

39. M. E. Rivera-Ramos, G. J. Ruiz-Mercado and A. J. Hernández-Maldonado, *Ind. Eng. Chem. Res.*, 2008, **47**, 5602-5610.

40. Q. Liu, N. C. O. Cheung, A. E. Garcia-Bennett and N. Hedin, *ChemSusChem*, 2011, **4**, 91-97.

41. R. M. Barrer, *J. Chem. Soc.*, 1948, 127-132.

42. D. W. Breck, *Zeolite molecular sieves: structure, chemistry, and use*, Wiley, 1973.

43. D. T. Hayhurst, *Chem. Eng. Commun.*, 1980, **4**, 729-735.

44. J. Janák, M. Krejčí and E. E. Dubský, *Ann. N. Y. Acad. Sci.*, 1959, **72**, 731-738.

45. J. Zhang, R. Singh and P. A. Webley, *Micro. Meso. Mater.*, 2008, **111**, 478-487.

46. F. N. Ridha, Y. Yang and P. A. Webley, *Micro. Meso. Mater.*, 2009, **117**, 497-507.

47. T. Inui, Y. Okugawa and M. Yasuda, *Ind. Eng. Chem. Res.*, 1988, **27**, 1103-1109.

48. G. C. Watson, N. K. Jensen, T. E. Rufford, K. I. Chan and E. F. May, *J. Chem. Eng. Data*, 2011, **57**, 93-101.

49. J. Shang, G. Li, R. Singh, Q. Gu, K. M. Nairn, T. J. Bastow, N. Medhekar, C. M. Doherty, A. J. Hill, J. Z. Liu and P. A. Webley, *J. Am. Chem. Soc.*, 2012, **134**, 19246-19253.

50. J. Shang, G. Li, R. Singh, P. Xiao, J. Z. Liu and P. A. Webley, *J. Phys. Chem. C*, 2013, **117**, 12841-12847.

51. D. W. Breck, W. G. Eversole, R. M. Milton, T. B. Reed and T. L. Thomas, *J. Am. Chem. Soc.*, 1956, **78**, 5963-5972.

52. R. J. Harper, G. R. Stifel and R. B. Anderson, *Can. J. Chem.*, 1969, **47**, 4661-4670.

53. M. Palomino, A. Corma, F. Rey and S. Valencia, *Langmuir*, 2009, **26**, 1910-1917.

54. Y. Delaval and E. C. de Lara, *J. Chem. Soc., Faraday Trans 1*, 1981, **77**, 869-877.

55. O. Cheung, Z. Bacsik, Q. Liu, A. Mace and N. Hedin, *Appl. Energy*, 2013, **112**, 1326-1336.

56. A. Mace, N. Hedin and A. Laaksonen, *J. Phys. Chem. C*, 2013, **117**, 24259-24267.

57. A. V. Larin, A. Mace, A. A. Rybakov and A. Laaksonen, *Micro. Meso. Mater.*, 2012, **162**, 98-104.

58. A. Mace, K. Laasonen and A. Laaksonen, *Phys. Chem. Chem. Phys.*, 2014, **16**, 166-172.

59. E. Jaramillo and M. Chandross, *J. Phys. Chem. B*, 2004, **108**, 20155-20159.

60. D. M. Ruthven, *Micro. Meso. Mater.*, 2012, **162**, 69-79.

61. D. M. Ruthven, *Adsorpt.*, 2001, **7**, 301-304.

62. H. Yucel and D. M. Ruthven, *J. Colloid Interface Sci.*, 1980, **74**, 186-195.

63. H. Yucel and D. M. Ruthven, *J. Chem. Soc., Faraday Trans 1*, 1980, **76**, 60-70.

64. E. F. Kondis and J. S. Dranoff, *Ind. Eng. Chem. Proc. Des. Dev.*, 1971, **10**, 108-114.

65. S. Araki, Y. Kiyohara, S. Tanaka and Y. Miyake, *J. Colloid Interface Sci.*, 2012, **388**, 185-190.

66. Y. Lee, J. A. Hriljac, T. Vogt, J. B. Parise, M. J. Edmondson, P. A. Anderson, D. R. Corbin and T. Nagai, *J. Am. Chem. Soc.*, 2001, **123**, 8418-8419.

67. D. R. Corbin, L. Abrams, G. A. Jones, M. M. Eddy, G. D. Stucky and D. E. Cox, *J. Chem. Soc., Chem. Commun.*, 1989, 42-43.

68. D. R. Corbin, L. Abrams, G. A. Jones, M. M. Eddy, W. T. A. Harrison, G. D. Stucky and D. E. Cox, *J. Am. Chem. Soc.*, 1990, **112**, 4821-4830.

69. T. M. Nenoff, J. B. Parise, G. A. Jones, L. G. Galya, D. R. Corbin and G. D. Stucky, *J. Phys. Chem.*, 1996, **100**, 14256-14264.

70. J. B. Parise and D. E. Cox, *J. Phys. Chem.*, 1984, **88**, 1635-1640.

71. J. B. Parise, L. Abrams, J. D. Jorgensen and E. Prince, *J. Phys. Chem.*, 1984, **88**, 2303-2307.

72. R. M. Barrer and E. V. T. Murphy, *J. Chem. Soc. A*, 1970, 2506-2514.

73. G. Aguilar-Armenta, G. Hernandez-Ramirez, E. Flores-Loyola, A. Ugarte-Castaneda, R. Silva-Gonzalez, C. Tabares-Munoz, A. Jimenez-Lopez and E. Rodriguez-Castellon, *J. Phys. Chem. B*, 2001, **105**, 1313-1319.

74. R. W. Triebe and F. H. Tezel, *Gas. Sep. Pur.*, 1995, **9**, 223-230.

75. K. P. Lillerud and J. H. Raeder, *Zeolites*, 1986, **6**, 474-483.

76. W. Xingqiao and X. Ruren, *Stud. Surf. Sci. Catal.*, 1985, **24**, 111-118.

77. G. T. Kerr, *Science*, 1963, **140**, 1412.

78. T. Remy, S. A. Peter, L. Van Tendeloo, S. Van der Perre, Y. Lorgouilloux, C. E. A. Kirschhock, G. V. Baron and J. F. M. Denayer, *Langmuir*, 2013, **29**, 4998-5012.

79. T. R. Cannan, E. M. Flanigen, R. T. Gajek, B. M. Lok, C. A. Messina and R. L. Patton, ed. U. S. Patent, Union Carbide Corporation, United States, 1982.

80. B. M. Lok, C. A. Messina, R. L. Patton, R. T. Gajek, T. R. Cannan and E. M. Flanigen, *J. Am. Chem. Soc.*, 1984, **106**, 6092-6093.

81. S. T. Wilson, B. M. Lok, C. A. Messina, T. R. Cannan and E. M. Flanigen, *J. Am. Chem. Soc.*, 1982, **104**, 1146-1147.

82. R. Roldán, M. Sánchez-Sánchez, G. Sankar, F. J. Romero-Salguero and C. Jiménez-Sanchidrián, *Micro. Meso. Mater.*, 2007, **99**, 288-298.

83. X. T. Ren, N. Li, J. Q. Cao, Z. Y. Wang, S. Y. Liu and S. H. Xiang, *Appl. Catal., A*, 2006, **298**, 144-151.

84. E. Aubert, F. Porcher, M. Souhassou and C. Lecomte, *Acta Crystallogr., Sect. B*, 2003, **59**, 687-700.

85. J. Jänchen and H. Stach, *Energy Procedia*, 2012, **30**, 289-293.

86. S. Wilson and P. Barger, *Micro. Meso. Mater.*, 1999, **29**, 117-126.

87. S. G. Hedge, P. Ratnasamy, L. M. Kustov and V. B. Kazansky, *Zeolites*, 1988, **8**, 137-141.

88. V. R. Choudhary and S. Mayadevi, *Langmuir*, 1996, **12**, 980-986.

89.   Q. J. Chen, M. A. Springuel-Huet and J. Fraissard, *Chem. Phys. Lett.*, 1989, **159**, 117-121.

90.   M. A. Carreon, S. Li, J. L. Falconer and R. D. Noble, *J. Am. Chem. Soc.*, 2008, **130**, 5412-5413.

91.   S. R. Venna and M. A. Carreon, *Langmuir*, 2011, **27**, 2888-2894.

92.   A. G. Arévalo-Hidalgo, J. A. Santana, R. Fu, Y. Ishikawa and A. J. Hernández-Maldonado, *Micro. Meso. Mater.*, 2010, **130**, 142-153.

93.   M. Briend, R. Vomscheid, M. J. Peltre, P. P. Man and D. Barthomeuf, *J. Phys. Chem.*, 1995, **99**, 8270-8276.

94.   T. Takeguchi, W. Tanakulrungsank and T. Inui, *Gas. Sep. Pur.*, 1993, **7**, 3-9.

95.   S. Li, J. L. Falconer and R. D. Noble, *J. Membr. Sci.*, 2004, **241**, 121-135.

96.   J. C. Poshusta, V. A. Tuan, E. A. Pape, R. D. Noble and J. L. Falconer, *AIChE J.*, 2000, **46**, 779-789.

97.   S. Li, G. Alvarado, R. D. Noble and J. L. Falconer, *J. Membr. Sci.*, 2005, **251**, 59-66.

98.   S. Li, J. G. Martinek, J. L. Falconer, R. D. Noble and T. Q. Gardner, *Ind. Eng. Chem. Res.*, 2005, **44**, 3220-3228.

99.   S. Li, J. L. Falconer, R. D. Noble and R. Krishna, *Ind. Eng. Chem. Res.*, 2006, **46**, 3904-3911.

100.   X. Su, P. Tian, D. Fan, Q. Xia, Y. Yang, S. Xu, L. Zhang, Y. Zhang, D. Wang and Z. Liu, *ChemSusChem*, 2013, **6**, 911-918.

101.   M. L. Carreon, S. Li and M. A. Carreon, *Chem. Comm.*, 2012, **48**, 2310-2312.

102.   I. Deroche, L. Gaberova, G. Maurin, P. Llewellyn, M. Castro and P. Wright, *Adsorpt.*, 2008, **14**, 207-213.

103.   H. Maghsoudi, M. Soltanieh, H. Bozorgzadeh and A. Mohamadalizadeh, *Adsorpt.*, 2013, **19**, 1045-1053.

104.   S. Himeno, T. Tomita, K. Suzuki, K. Nakayama, K. Yajima and S. Yoshida, *Ind. Eng. Chem. Res.*, 2007, **46**, 6989-6997.

105.   M. Miyamoto, Y. Fujioka and K. Yogo, *J. Mater. Chem.*, 2012, **22**, 20186-20189.

106.   J. van den Bergh, W. Zhu, J. C. Groen, F. Kapteijn, J. A. Moulijn, K. Yajima, K. Nakayama, T. Tomita and S. Yoshida, in *Stud. Surf. Sci. Catal.*, eds. Z. G. J. C. Ruren Xu and Y. Wenfu, Elsevier, 2007, pp. 1021-1027.

107.   J. van den Bergh, W. Zhu, J. Gascon, J. A. Moulijn and F. Kapteijn, *J. Membr. Sci.*, 2008, **316**, 35-45.

108.   T. D. Pham, R. Xiong, S. I. Sandler and R. F. Lobo, *Micro. Meso. Mater.*, 2014, **185**, 157-166.

109.   A. Philippou and M. W. Anderson, *Zeolites*, 1996, **16**, 98-107.

110.   C. B. Lopes, M. Otero, J. Coimbra, E. Pereira, J. Rocha, Z. Lin and A. Duarte, *Micro. Meso. Mater.*, 2007, **103**, 325-332.

111.   C. B. Lopes, E. Pereira, Z. Lin, P. Pato, M. Otero, C. M. Silva, J. Rocha and A. C. Duarte, *Micro. Meso. Mater.*, 2011, **145**, 32-40.

112.   P. J. E. Harlick and F. H. Tezel, *Micro. Meso. Mater.*, 2004, **76**, 71-79.

113.   S. M. Kuznicki, V. A. Bell, S. Nair, H. W. Hillhouse, R. M. Jacubinas, C. M. Braunbarth, B. H. Toby and M. Tsapatsis, *Nature*, 2001, **412**, 720-724.

114.   V. A. Bell, D. R. Anderson, B. K. Speronello, M. Rai and W. B. Dolan, ed. U. S. Patent, 2006.

115.   S. M. Kuznicki, in *United States Patent*, ed. U. S. Patent, Engelhard Corporation, United States, 1989.

116.   S. W. Park, S. H. Cho, W. S. Ahn and W. J. Kim, *Micro. Meso. Mater.*, 2011, **145**, 200-204.

117.   A. Anson, C. C. H. Lin, S. M. Kuznicki and J. A. Sawada, *Chem. Eng. Sci.*, 2009, **64**, 3683-3687.

RSC Advances

Narrow pore sorbents

95x38mm (300 x 300 DPI)